



## An high resolution FDIRC for the measurement of cosmic-ray isotopic abundances

P.S. Marrocchesi, M.G. Bagliesi, K. Batkov, G. Bigongiari, M.Y. Kim, P. Maestro

### ► To cite this version:

P.S. Marrocchesi, M.G. Bagliesi, K. Batkov, G. Bigongiari, M.Y. Kim, et al.. An high resolution FDIRC for the measurement of cosmic-ray isotopic abundances. *Astroparticle Physics*, 2011, 35 (1), pp.21. 10.1016/j.astropartphys.2011.05.003 . hal-00769167

**HAL Id: hal-00769167**

**<https://hal.science/hal-00769167>**

Submitted on 29 Dec 2012

**HAL** is a multi-disciplinary open access archive for the deposit and dissemination of scientific research documents, whether they are published or not. The documents may come from teaching and research institutions in France or abroad, or from public or private research centers.

L'archive ouverte pluridisciplinaire **HAL**, est destinée au dépôt et à la diffusion de documents scientifiques de niveau recherche, publiés ou non, émanant des établissements d'enseignement et de recherche français ou étrangers, des laboratoires publics ou privés.

## Accepted Manuscript

An high resolution FDIRC for the measurement of cosmic-ray isotopic abundances

P.S. Marrocchesi, M.G. Bagliesi, K. Batkov, G. Bigongiari, M.Y. Kim, P. Maestro

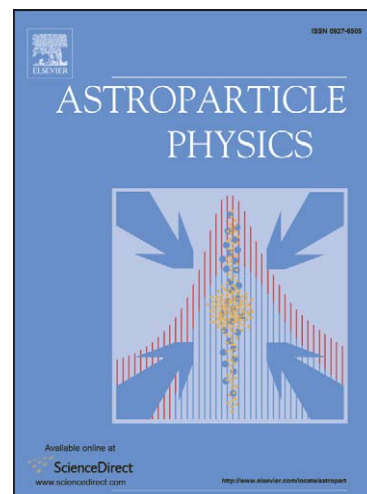
PII: S0927-6505(11)00087-9  
DOI: [10.1016/j.astropartphys.2011.05.003](https://doi.org/10.1016/j.astropartphys.2011.05.003)  
Reference: ASTPHY 1595

To appear in: *Astroparticle Physics*

Received Date: 26 February 2011  
Revised Date: 10 April 2011  
Accepted Date: 5 May 2011

Please cite this article as: P.S. Marrocchesi, M.G. Bagliesi, K. Batkov, G. Bigongiari, M.Y. Kim, P. Maestro, An high resolution FDIRC for the measurement of cosmic-ray isotopic abundances, *Astroparticle Physics* (2011), doi: [10.1016/j.astropartphys.2011.05.003](https://doi.org/10.1016/j.astropartphys.2011.05.003)

This is a PDF file of an unedited manuscript that has been accepted for publication. As a service to our customers we are providing this early version of the manuscript. The manuscript will undergo copyediting, typesetting, and review of the resulting proof before it is published in its final form. Please note that during the production process errors may be discovered which could affect the content, and all legal disclaimers that apply to the journal pertain.



## An high resolution FDIRC for the measurement of cosmic-ray isotopic abundances

P. S. Marrocchesi<sup>\*a</sup>, M. G. Bagliesi<sup>a</sup>, K. Batkov<sup>a</sup>, G. Bigongiari<sup>a</sup>, M. Y. Kim<sup>b</sup>, P. Maestro<sup>a</sup><sup>a</sup>Dept. of Physics, University of Siena and INFN, V. Roma 56, 53100 Siena (Italy)<sup>b</sup>INFN sez. di Pisa, Largo B. Pontecorvo 3, 56127 Pisa (Italy)**Abstract**

Measurements of the relative abundance of cosmic isotopes and of the energy dependence of their fluxes may clarify our present understanding on the confinement time of charged cosmic rays in the Galaxy. Experimental studies of these *propagation clocks* have been carried out by balloon and space missions at energies of a few 100 MeV/amu by means of detection techniques based on multiple dE/dx sampling, coupled with a measurement of the energy released in a thick absorber. At larger energies, the isotopic separation of light nuclei (as, for instance,  $^9\text{Be}/^{10}\text{Be}$ ) can be achieved by combining a precise measurement of the particle's rigidity with an high resolution determination of its velocity, via the observation of the Cherenkov effect in a radiator.

In this paper, we propose the introduction – for the first time in a space experiment – of the DIRC technique (Detection of Internal Reflected Cherenkov light) for the identification of cosmic-ray isotopes. This type of detector has been successfully used in electron-positron colliders for particle identification and in particular for  $\pi$ -K separation. While for particles with unit charge the light yield is a limiting factor, in the case of a nucleus of charge  $Z$  the larger photostatistics (due to the  $Z^2$  dependence of Cherenkov light emission) is the key to reach an adequate angular resolution to provide a mass discrimination for isotopes of astrophysical interest. We report on the early development phase of a DIRC prototype with a focussing scheme (FDIRC) to collect the Cherenkov light onto a detector plane instrumented with a Silicon PhotoMultiplier (SiPM) array.

**Key words:** cosmic-ray isotopes, particle identification, Silicon PhotoMultiplier, FDIRC

**1. Introduction**

In addition to stable nuclei, the cosmic-ray flux includes radioactive nuclides of primary and secondary origin. Secondary isotopes undergoing  $\beta^\pm$  decay can provide important information about the confinement time of cosmic rays, i.e. the average time spent during their diffusive propagation inside the Galaxy. From the observed residual fraction of  $^{10}\text{Be}$  (a  $\beta^-$  emitter with a mean life of about  $1.5 \times 10^6$  years), a confinement time of order  $10^7$  years has been estimated [1]. The measurement of the  $^9\text{Be}/^{10}\text{Be}$  abundance ratio provides a confinement time dominated by the propagation history of the C, N, O group. It is interesting to compare this result with the one provided by heavier elements, as for instance  $^{26}\text{Al}$ ,  $^{36}\text{Cl}$ .

The instrument CRIS (Cosmic-Ray Isotope Spectrometer), aboard the Cosmic Explorer (ACE) launched by NASA in 1997 and inserted into the L1 Lagrangian point, can identify isotopes in the interval  $Z=2$  to  $Z=30$  with a geometrical factor of about  $250 \text{ cm}^2\text{sr}$  and an excellent mass resolution [2]. The detection technique used by CRIS (multiple dE/dx measurements vs. range) limits to about 500 MeV/nucleon the energy span of the experiment.

An excellent isotopic separation of the radioactive  $^{10}\text{Be}$  versus its stable neighbor  $^9\text{Be}$  was achieved – up to energies

of about 2 GeV/amu – by the balloon-borne spectrometer ISOMAX [3] with simultaneous measurements of the velocity and rigidity of the incoming nucleus.

In this paper, we propose – for the first time to our knowledge – the use in a space mission of a high resolution FDIRC detector to achieve the required angular resolution for the measurement of the isotopic abundances in the flux of cosmic radiation at energies of a few GeV/amu. The idea originates from the large advantage that fully ionized nuclei provide in terms of photostatistics, due to the  $Z^2$  dependence of the Cherenkov light yield. Differently from experiments at colliders, where the DIRC technique is applied to the detection of  $Z=1$  particles, in this case the contribution to the angular error due to the available photostatistics can be reduced by almost one order of magnitude.

The proposed high resolution FDIRC would also allow for a very compact design of a barrel-type detector for particle identification in experiments at colliding beams.

**2. Mass separation requirements**

A measurement of the particle velocity  $\beta$  coupled to a precise measurement of its momentum  $P$  with a magnetic spectrometer, results in a mass  $M$  resolution given by:

$$\left(\frac{\sigma_M}{M}\right)^2 = \left(\frac{\sigma_P}{P}\right)^2 + \left(\gamma^2 \frac{\sigma_\beta}{\beta}\right)^2 \quad (1)$$

<sup>\*</sup>corresponding author: marrocchesi@pi.infn.it

where  $\gamma$  is the Lorentz factor. The discrimination between two relativistic isotopes with the same magnetic rigidity and mass numbers  $A$  and  $A+1$ , respectively, can be achieved by a measurement of the angular separation  $\Delta\theta_c$  in the Cherenkov angle  $\theta_c$  given by:

$$\Delta\theta_c = \frac{(1 + 2A) m_n^2}{2 A^2 P_n^2 \tan \theta_c} \sim \frac{m_n^2}{A P_n^2 \sqrt{n^2 - 1}} \quad (A \gg 1) \quad (2)$$

where  $m_n$  is the atomic mass unit,  $P_n$  is the momentum per nucleon and  $n$  is the index of refraction of the radiator.

In Table 1, we list the angular separation between a few selected isotopes of astrophysical interest with a rigidity of 6.2 GV and 7.9 GV, respectively. For the latter rigidity value, the tightest requirement on the angular resolution is of the order of 0.3 mrad (for a  $5\sigma$  separation of  $^{40}\text{Ca}$  and  $^{41}\text{Ca}$ ), while for lighter nuclei like Be an angular resolution of about 1 mrad is adequate.

The requirements for the measurement of the magnetic rigidity are discussed in the last paragraph.

### 3. An FDIRC with SiPM based photodetection

The development of a differential Cherenkov detector, known as DIRC (Detection of Internally Reflected Cherenkov light), started with the BaBar experiment at SLAC [4], where it was successfully operated as a particle identifier (PID) achieving a suitable ( $> 3\sigma$ )  $\pi$ -K mass separation for momenta up to 3 – 4 GeV/c. The Cherenkov light, generated by the passage of a charged particle in a fused silica bar (an artificial and not crystalline type of quartz), propagates via multiple internal reflections along the radiator. After reaching one end of the bar, the light crosses a standoff volume filled with water and it is finally detected on a plane instrumented with an array of photomultipliers. From the projected image onto the detector plane, one can derive the aperture of the Cherenkov cone (Fig. 1), taking advantage of the tracking information on the direction of incidence of the particle.

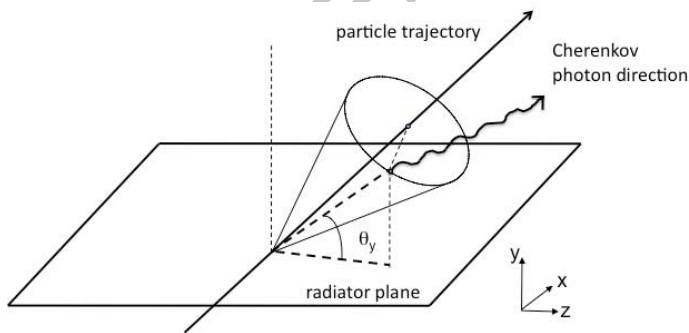


**Figure 1:** Definition of the  $\theta_y$  angle between the Cherenkov photon direction and the radiator plane. This angle is conserved during the light propagation along the bar and will be used throughout the paper as the measured quantity. For tracks at normal incidence, the Cherenkov half cone angle is the complementary angle:  $\pi/2 - \theta_y$ .

The introduction of a focalization scheme of the light emitted at one end of the radiator (Fig. 2) represents the next step in the development of this type of detector, known as Focussing DIRC or FDIRC [5]. The main advantages of the focussing technique include the drastic reduction of the so called “pinhole effect” [6], whereby the Cherenkov image on the detection plane is broadened in proportion to the size of the exit aperture of the radiator bar; the reduction of the standoff distance (from about 1 m, as in the case of BaBar, to about 10 cm or less); a more uniform coverage of the focal plane with a smaller total number of photodetectors.

The FDIRC concept has been applied to the design of end-cap detectors (where the radiator has a disc-like shape) in the case of the experiments BELLE at KEK [10] and PANDA at FAIR [7, 8], as well as the proposed design for a SuperB particle identification detector [9].

In the example of [10], the focalization scheme is based on a Focussing Block (FB) including two reflecting surfaces (a flat mirror and a toroidal mirror) with dimensions of the order of 10 cm, shaped from a single block of fused silica (the same material of the radiator). In this case, the focal plane is subdivided into square pixels with size of the order of 1 mm ( $\Delta\theta_y = 1^\circ$ ) along the vertical coordinate, related to the Cherenkov angle, and about 30 mm for the measurement of the azimuthal angle ( $\Delta\phi = 3^\circ$ ).

A fine granularity of 1 mm was obtained by instrumenting the focal plane with an array of optical fibers connected to Multi-Anode Photomultipliers (MAPMT). However, in this implementation, the light collection efficiency is quite modest ( $\sim 10\%$ ) due to the limited numerical aperture and packing fraction ( $\sim 60\%$ ) of the fibers.

This important limitation can be overcome – as described in this paper – with the use of solid state photosensors known as Silicon PhotoMultiplier (SiPM).

The Silicon PhotoMultiplier [11, 12] is a novel solid-state photon counting device. It consists of a matrix of Avalanche PhotoDiodes operating in the Geiger regime with resistive quenching and connected in parallel into a single readout element. This solution allows for a simplification of the scheme based on MAPMTs coupled to fibre bundles. In addition to their superior photon-counting capability, SiPM devices can operate in a magnetic field, while conventional photomultipliers may require a magnetic shield and/or a proper orientation of the tube axis with respect to the field lines. The possibility of an independent measurement of the Time of Propagation (TOP) along the radiator bar, with a time resolution not larger than 100 ps, is the basis of the TOP-DIRC concept [13]. In this case too, the utilization of SiPM photosensors might be of advantage, given their excellent time response.

#### 3.1. Main factors affecting the angular resolution

The angular spread  $\Delta\theta_y$  of the image on the focal plane depends on several factors [6]:

| $\Delta\theta$ (mrad)                 | 6.2 GV | 7.9 GV |
|---------------------------------------|--------|--------|
| ${}^9\text{Be} - {}^{10}\text{Be}$    | 11.2   | 6.9    |
| ${}^{26}\text{Al} - {}^{27}\text{Al}$ | 3.0    | 1.8    |
| ${}^{35}\text{Cl} - {}^{36}\text{Cl}$ | 2.3    | 1.4    |
| ${}^{40}\text{Ca} - {}^{41}\text{Ca}$ | 1.9    | 1.2    |
| ${}^{53}\text{Mn} - {}^{55}\text{Mn}$ | 3.3    | 2.0    |
| ${}^{54}\text{Fe} - {}^{56}\text{Fe}$ | 3.1    | 1.9    |
| ${}^{58}\text{Ni} - {}^{60}\text{Ni}$ | 2.9    | 1.8    |

**Table 1:** Cherenkov angle separation (in mrad) between some isotopes of astrophysical interest with the same rigidity  $R = 6.2$  GV (left) and 7.9 GV (right), respectively. The calculation assumes a refractive index ( $n = 1.55$ ) as representative of an average value over the wavelength interval covered by the proposed instrument.

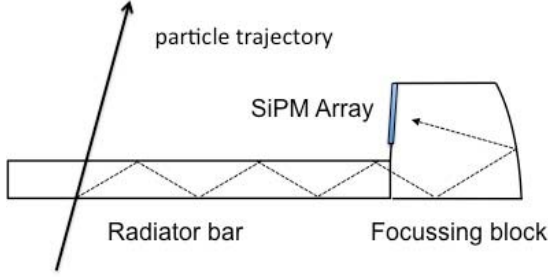


**Figure 2:** Conceptual scheme of the prototype FDIRC with focussing block and focal plane equipped with SiPM photosensors.

- the “pinhole effect” due to the size of the exit window of the radiator bar;
- the angular dispersion due to geometrical imperfections of the radiator (propagation smearing);
- the chromatic dispersion along the whole optical path;

Other (usually minor) contributions include:

- the effect of  $\delta$  rays;
- the effect of multiple scattering in the radiator;
- the uncertainty on the track direction due to the tracking system;
- the discretization error due to the pixel size on the focal plane

The angular resolution is strongly affected by photostatistics, i.e. the effective number of photoelectrons  $N_{pe}$  available for the determination of the centroid of the image on the focal plane. Let  $\sigma(\theta_i)$  be the angular spread due to a *single photoelectron*. The error on the Cherenkov angle  $\theta_y$  from the fitted value of the centroid of the distribution on the focal plane is given by:

$$\sigma(\theta_y) = \frac{\sigma(\theta_i)}{\sqrt{N_{pe}}} + C \quad (3)$$

where the constant term  $C$  includes the contribution of systematic uncertainties.

If we consider the above contributions to  $\sigma(\theta_i)$ , we find that the error due to the “pinhole” effect can be strongly reduced with the introduction of a focussing scheme; the error due to the spatial discretization can be made negligible by a suitable choice of the pixel dimension, while the irreducible contribution due to the geometrical imperfections of the radiator can only be realistically reduced to  $\sigma(\theta_i) = 2 - 4$  mrad *per photoelectron* [14].

The chromatic dispersion can also be an important cause of degradation of the angular resolution. This contribution is of the order of  $\sigma(\theta_i) \sim 5.4$  mrad *per photoelectron* in BaBar [4] and it is particularly relevant for tracks at normal incidence on the radiator, as they produce the largest number of multiple internal reflections. However, given the large gain in photostatistics due to the  $Z^2$  factor, we plan to restrict our window for photodetection to the spectral interval 400–600 nm in order to avoid the larger chromatic dispersion in the ultraviolet band.

An alternative scheme of chromatic correction is based on a dispersive element, as proposed by the experiment PANDA, where a LiF plate is optically coupled to a focussing light guide [7].

### 3.2. Monte Carlo simulation with a cylindrical mirror

At present, our research group is developing an high resolution FDIRC prototype with a focal plane instrumented with an array of SiPM sensors. In the Monte Carlo simulation reported below, we assume a segmentation into pixels of  $5 \text{ mm} \times 0.5 \text{ mm}$  size.

For the proposed configuration, the dominant contribution to the angular distribution is due to photostatistics. Assuming an average loss of 15% on the mirrors and a Photon Detection Efficiency (PDE) of order 50% (optimized in the spectral interval 400–600 nm), the expected number of Cherenkov photoelectrons per unit thickness of the radiator is  $N_{pe} \sim 38 \text{ cm}^{-1}$  (for  $Z=1$ ). This number increases to about  $600 \text{ cm}^{-1}$  in the case of Be ( $Z=4$ ), thus allowing for a reduction of a factor close to 4 of the statistical error on the centroid of the



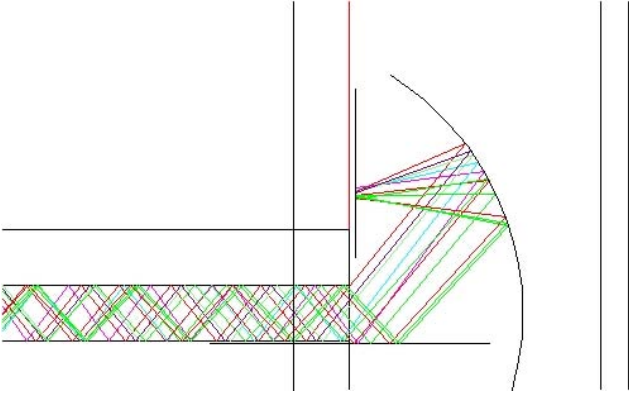


**Figure 3:** Example of ray-tracing inside the radiator bar and focalization with a cylindrical mirror on the detector plane.

distribution (the error decreases as  $1/Z$ ).

We carried out a Monte Carlo simulation of our FDIRC concept, with the FLUKA package [15], by generating events where relativistic ions impinge on a 10 mm thick bar of fused silica. A full simulation (ray-tracing) covers the whole optical path of the generated Cherenkov light, first transported along the bar by total internal reflection, then focussed by a reflecting surface (placed at about 10 cm from the end of the bar) on a detector plane, structured into pixels (Fig. 3). In this case, the focalization acts only in one dimension, along the  $y$  axis, and it is implemented with a cylindrical mirror.

The distributions in Fig. 4 refer to 1000 events of  $^{10}\text{Be}$  nuclei with 2.35 GeV/amu kinetic energy, generated at normal incidence on the radiator: (a) the total number of photons collected on the focal plane in the spectral interval 400 – 600 nm is of the order of  $1500 \text{ cm}^{-1}$  (neglecting mirror losses); (b) the fitted angle  $\theta_y$  on the focal plane (i.e.: the complementary of the Cherenkov semi-aperture angle) is close to 400 mrad, as expected taking into account the demagnification ratio due to the focussing. The angular resolution on the reconstructed angle is close to 1 mrad.

In this simulation, all pixels have the same size ( $5 \text{ mm} \times 0.5 \text{ mm}$ ) and the average pixel occupancy in the central region ( $-5 \text{ cm}, +5 \text{ cm}$ ) is between 10 and 35 photons, as shown in Fig. 5. For each event, the spatial distribution of photons collected on the focal plane is fitted with an hyperbola and the original Cherenkov angle is reconstructed. One example is shown in Fig. 6.

Two samples of events of  $^9\text{Be}$  and  $^{10}\text{Be}$  nuclei with the same rigidity were generated hitting the bar (at normal incidence) at a distance of 10 cm from its end. The reconstructed Cherenkov angles (Fig. 7) show an angular difference close to 6 mrad and an angular resolution of about 1.1 mrad, corresponding to a  $5.6 \sigma$  separation, approximately.

In our estimate, we assumed to filter off the UV part of

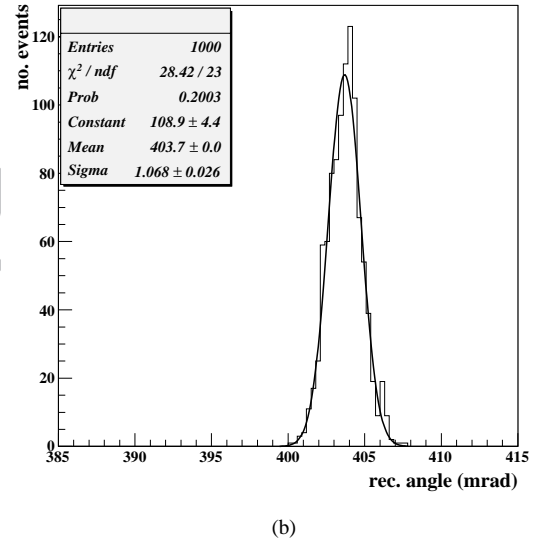
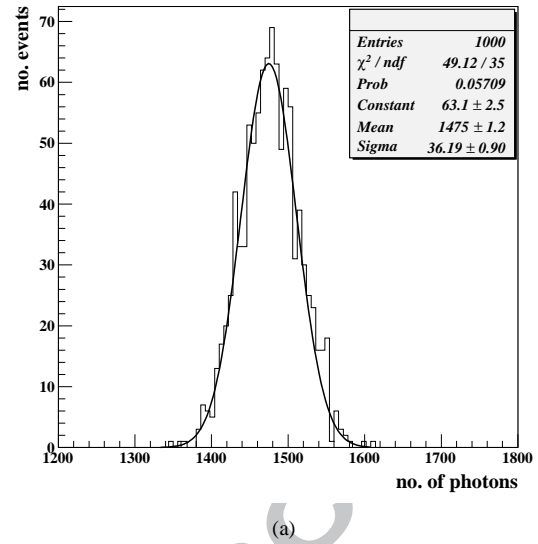
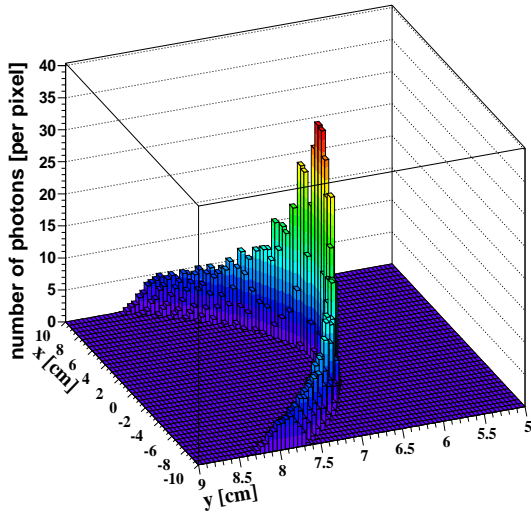


**Figure 4:**  $^{10}\text{Be}$  nuclei (2.35 GeV/amu) at normal incidence on the radiator in our simulation by FLUKA: (a) total number of photons collected on the focal plane in the spectral interval 400 – 600 nm; (b) reconstructed Cherenkov angle  $\theta_y$  on the focal plane. Taking into account the demagnification ratio, the  $\theta_y$  angle at the bar exit is close to 737 mrad.

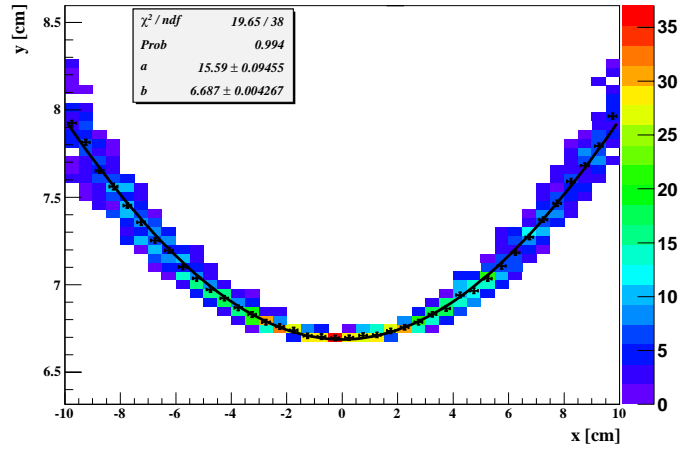
the Cherenkov spectrum where the chromatic dispersion is larger. The simulation does not take into account of propagation smearing due to imperfections in the geometry of the radiator.

### 3.3. Toroidal mirror and pixel size optimization

The next step in our design study has been the simulation of an optical scheme to allow for the focussing of the Cherenkov light, at the exit of the bar, not only in the vertical but also in the horizontal plane. The goal was to reduce the sensitive area to be instrumented with photosensors on the focal plane.



(a)



(b)

**Figure 5:**  $^{10}\text{Be}$  nuclei (2.35 GeV/amu) at normal incidence on the radiator: distribution of the number of photons collected by each pixel on the focal plane.

A toroidal mirror with radii  $R_y = 22$  cm ( $R_x = 14$  cm), for the focalization in the vertical (horizontal) plane, was simulated at a distance of about 10 cm from the end of the bar. The image shown in Fig. 8 refers to a single Monte Carlo event resulting from the superposition of the Cherenkov patterns generated, respectively, by one  $^9\text{Be}$  and one  $^{10}\text{Be}$  track with the same rigidity (6.2 GV), both at normal incidence and with the same impact coordinate along the bar. In this simulation, the pixel size was 4 mm  $\times$  0.2 mm, along x and y respectively. The two Cherenkov patterns on the focal plane are clearly separated.

Optimization of the pixel size along the y-axis results from a tradeoff between a segmentation with a sufficiently small granularity to achieve the required angular separation and the constraint that the average number of photoelectrons, generated by any pixel hit by the Cherenkov light, should be not too small compared to the expected background level of the photosensor. In principle, a typical SiPM threshold of 1.5 to 2.5 p.e. would be necessary to reduce the SiPM dark count rate at room temperature to an acceptable level. However, the threshold can be lowered even below the single photoelectron, provided the time of arrival of each photon is recorded (as explained in paragraph (ii) of section 4) and an offline selection is applied, rejecting all spurious hits outside a narrow “time-window” around the occurrence of the Cherenkov event.

The size of the pixels along the x-axis is less critical for the angular resolution and the presence of dead zones as large as 1 mm at the boundary between one “column” (64 pixels along the y-direction) and an adjacent one can be tolerated. Our final choice for the pixel size was 4 mm  $\times$  0.2 mm.

**Figure 6:** Fit of a single Cherenkov event generated by a  $^{10}\text{Be}$  nucleus (2.35 GeV/amu) at normal incidence on the radiator. Pixel size is 5 mm along the abscissa and 0.5 mm along the y-axis.

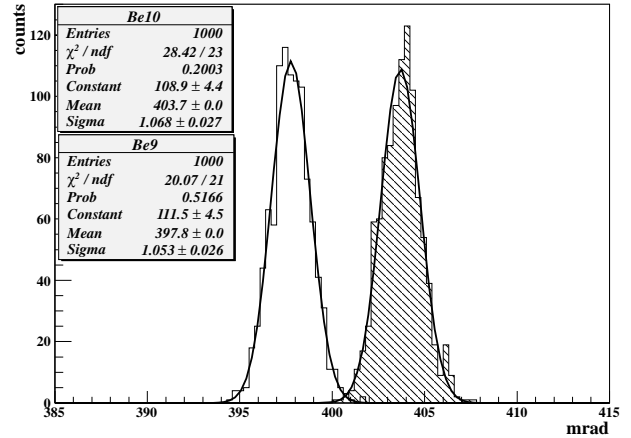


**Figure 7:** Reconstructed angles from Monte Carlo samples of  $^9\text{Be}$  and  $^{10}\text{Be}$  (filled histogram) nuclei with 31.5 GeV/c particle momentum. The corresponding kinetic energies per nucleon are 2.7 GeV/amu and 2.35 GeV/amu, respectively. Here again the  $\theta_y$  angles are measured on the focal plane. Taking into account the demagnification ratio, the  $\theta_y$  angle of  $^{10}\text{Be}$  is close to 737 mrad at the bar exit.

### 3.4. Effects due to the incidence angle of the track

Incident tracks were simulated, not only at normal incidence to the bar, but also as a combination of the two rotations described in Fig. 9. In particular, rotations around the x-axis (tilt-x) generate an hyperbolic geometrical pattern on the focal plane that gets displaced towards the negative values of the y-coordinate with increasing (absolute) values of the rotation angle. In order to be able to reconstruct tracks with tilt-x angles in the range  $[-30^\circ, +30^\circ]$  the instrumented area on the focal plane – in our geometry – should be close to 4 cm  $\times$  4 cm, according to our simulations.

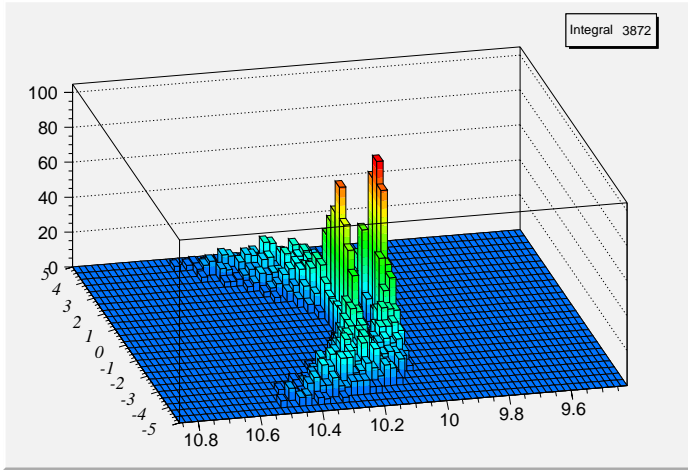


**Figure 8:** Example of the superposition on the focal plane of two Cherenkov patterns generated via Monte Carlo by one  $^9\text{Be}$  and one  $^{10}\text{Be}$  tracks both with a total particle momentum of 25 GeV/c.

For tilt angles larger than about  $\pm 8^\circ$  light losses are expected whenever the Cherenkov light hits an internal wall of the bar at an angle that does not satisfy the condition for internal reflection.

Optimization studies on the design of the focussing optics (the toroidal mirror is not the only viable option) are being carried out in the direction to reduce the overall size of the focussing block and of the sensitive area on the focal plane and to minimize the light losses at oblique track incidence.

#### 4. Prototype development

SiPM photosensors [16, 17] offer a number of advantages including: single-photon sensitivity; large Photon Detection Efficiency (PDE); tolerance to magnetic fields; low bias voltage; low material budget; ruggedness. On the other hand, this device suffers from two main problems: (i) a dependence of the gain on the temperature; (ii) a large dark count rate at room temperature.

(i) In order to mitigate the problem of the temperature dependence of the gain (e.g.: about a factor 0.2 / $^\circ\text{C}$ ) a strict control of the temperature (at the level of a few tens of mK) is required. An alternative solution is to implement an active gain control by means of a linear feed-back on the bias voltage, based on a temperature measurement. Our research group accumulated a long working experience with SiPM devices with sensitive areas of 1 mm<sup>2</sup> [18] and 3 mm  $\times$  3 mm. By applying an active gain control scheme, we achieved a gain stabilization to about 1% in a long duration test while the device was operated under controlled temperature cycles [19].

(ii) To reduce the dark count rate – without relying on cryogenic temperatures – we implemented custom front-end electronics for SiPM readout with auto-trigger capability, where the pulse height information from the photosensor can

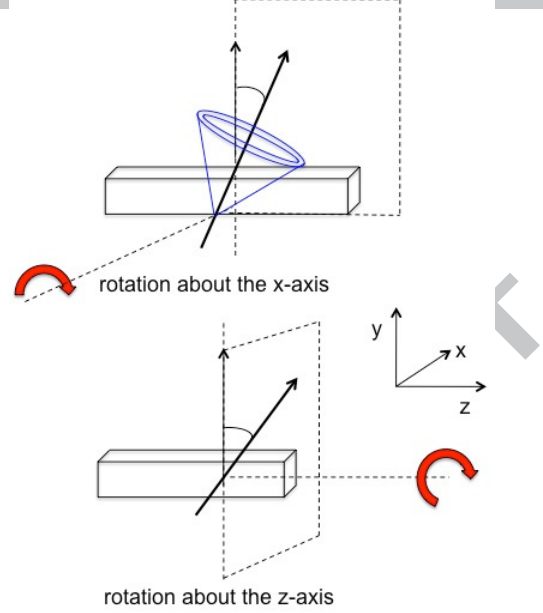


**Figure 9:** Definition of the tilt angles of the incident track with respect to the bar axes.

be selected inside a tight (1-2 ns) time-window around the Cherenkov event. This was made possible by the development of a custom ASIC (Application Specific Integrated Circuit), with 64 channels, carried out in collaboration with GM-Ideas, Norway [20].

A readout board – developed by our group [21] – with a 16 bit ADC and interfaced via the USB2 protocol to a PC, records both the pulse height of each fired channel and a time stamp generated when the signal crosses an individually adjustable threshold. The pulse height spectrum recorded with this board from an 1mm  $\times$  1mm SiPM (Hamamatsu S10362-11-050C) illuminated with a blue LED is shown in Fig. 10, where individual photo-peaks are clearly resolved.

According to our current FDIRC prototype design, the focal plane will be instrumented with a mosaic of 8 to 16 SiPM arrays. The latter are seamless linear arrays of 64 SiPM where each photosensors has an active area of 4 mm  $\times$  200  $\mu\text{m}$  each and it is structured into 320 elementary Geiger cells of 50  $\mu\text{m}$  size.

Each array is connected to the 64 channels of the front-end ASICs. According to the current design, an area on the focal plane of about 4.2 cm  $\times$  1.3 cm will be covered by 1024 pixels and readout by 16 ASICs. This number might be reduced by a factor of two with a suitable ganging scheme.

#### 5. Requirements for the rigidity measurement

An high resolution measurement of the Cherenkov angle will allow isotope identification for a given value of the particle's rigidity. The latter has to be measured independently (e.g: with a magnetic spectrometer) and at a level of accuracy that can be



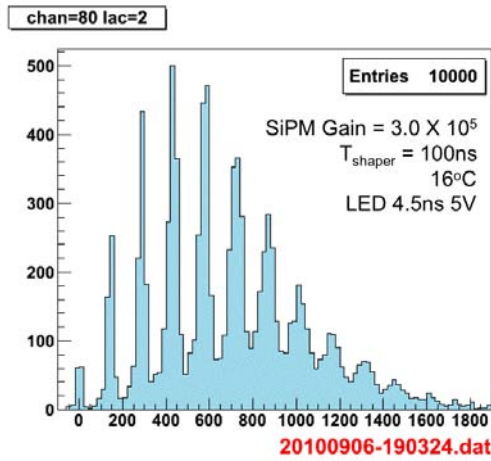


**Figure 10:** Measured photoelectron spectrum obtained in our laboratory with a  $1\text{ mm} \times 1\text{ mm}$  SiPM illuminated with a blue LED.

estimated from eq. (1).

If we consider – as an example – the case of the separation of  $^9\text{Be}$  and  $^{10}\text{Be}$  nuclei for kinetic energies above the Cherenkov threshold ( $\sim 300\text{ MeV/amu}$ ) in a radiator of Fused Silica (with an average index of refraction  $\sim 1.55$  in the wavelength range we have chosen) we can easily see that a mass separation at  $5\sigma$  level requires a mass resolution of  $0.2\text{ amu}$  and therefore a relative error on the reconstructed mass not larger than  $2\%$ . This sets an upper limit to the error on the momentum measurement.

In the case of a magnetic spectrometer, multiple scattering (MS) is typically the dominant term at these energies and care in the design of the spectrometer should be taken to minimize the amount of material traversed by the particle. While for ground experiments it is relatively straightforward to provide a momentum measurement dominated, at momenta of a few  $\text{GeV/c}$ , by a multiple scattering contribution to  $\Delta p/p$  of the order of  $0.3\%$  – as it is the case for most gas volume trackers, like for instance Time Projection Chambers – for experiments in space or on a balloon the problem is much more challenging. In this case, solid-state position detectors or fiber trackers are the typical choice while the use of gas-based detectors is technically difficult to implement especially for long duration missions. However, a design of spectrometers with cutting-edge technology (e.g.: Si trackers, or fiber trackers as in the case of the proposed balloon-borne PEBS-2 experiment [22]) allows for a momentum resolution dominated by a constant MS contribution that can be kept below  $2\%$  for particle momenta up to  $20 - 40\text{ GeV/c}$ .

Once this requirement is fulfilled, the quadratic dependence on the particle momentum of the second term in eq. (1) sets an upper limit to the maximum kinetic energy where isotope separation can be carried out. Taking into account the  $\sin^2\theta$  dependence of the Cherenkov light yield, we can predict the expected photostatics available for a given rigidity and the corresponding angular resolution. Our present estimate is that a separation

$> 3\sigma$  can be carried out for  $^9\text{Be}/^{10}\text{Be}$  up to a kinetic energy of about  $4\text{ GeV/amu}$  with an FDIRC radiator of  $10\text{ mm}$  thickness and a Cherenkov wavelength window from  $400$  to  $600\text{ nm}$ . Improvements on this upper limit are not to be excluded.

## 6. Conclusions

We introduced the concept of an FDIRC with a finely segmented focal plane instrumented with SiPM photosensors. This detector is designed to provide an high resolution measurement of the Cherenkov angle for charged nuclei crossing a radiator bar. Coupled to an independent measurement of the particle's rigidity, this instrument can achieve the required resolution to separate individual isotopes of astrophysical interest in the flux of cosmic rays.

It is perhaps not unreasonable to imagine that the development of the instrument described in this paper – in terms of a compact design of the optics and readout electronics – might lead to the concept of a space instrument, designed for cosmic isotopes abundance measurements, covering an active area of the order of  $1\text{ m}^2$  and placed “below” a dedicated magnetic spectrometer.

## 7. Acknowledgements

This work is part of the R&D program SPIDER funded by the Istituto Nazionale di Fisica Nucleare (INFN) in Italy.

## References

- [1] M.E. Wiedenbeck and D.E. Greiner, D. E, A Cosmic-Ray Age Based on the Abundance of  $^{10}\text{Be}$ , *Astrophys. J.* 239 (1980) 139
- [2] E. C. Stone et al., The Cosmic-Ray ISotope spectrometer for the Advanced Composition Explorer, *Space Science Reviews* 96 (1998) 285
- [3] T. Hams et al., *ApJ* 611 (2004) 892
- [4] I. Adam et al., *Nucl. Instrum. Meth. A* 538 (2005) 281
- [5] T. Kamae et al., Focussing DIRC as the Particle Identifier for the Forward End-Cap and Barrel Regions, *BELLE Note* 49, January 1995
- [6] B.N.Ratcliff, *Nuclear Instruments and Methods in Physics Research A* 502 (2003) 211
- [7] K. Föhl et al., *Nucl. Instrum. Meth. A* 595 (2008) 88
- [8] K. Föhl et al., The focussing-lightguide Disc DIRC design, *Proc. of the Workshop on fast Cherenkov detectors Photon detection, DIRC design and DAQ*, Giessen, Germany, May 1113 2009
- [9] J. Vavra, Focusing DIRC design for Super B, *SLAC-PUB-13763* October 27, 2009 (Addendum on December 15, 2009)
- [10] T. Kamae et al., *Nucl. Instrum. Meth. A* 382 (1996) 430
- [11] P.Buzhan et al., *Nucl.Instr. and Meth. A* 504 (2003) 48
- [12] V. Saveliev and V. Golovin, *Nucl.Instr. and Meth. A* 442 (2000) 223
- [13] C. Field et al., *Nucl. Instr. and Meth. A* 553 (2005) 96
- [14] J. Cohen-Tanugi et al., Optical Properties of the DIRC Fused Silica Cherenkov Radiator, *SLACPUB9735*, 2003
- [15] A. Ferrari, P.R. Sala, A. Fassò, J. Ranft, FLUKA: a multi-particle transport code, *CERN* – 2005 – 10, 2005.
- [16] N.Dinu et al., *Nucl.Instrum.and Meth. A* 572 (2007) 422
- [17] V. Golovin et al., *Nucl.Instr. and Meth. A* 518 (2004) 560
- [18] P.S. Marrocchesi et al., Test of front-end electronics with large dynamic range coupled to SiPM for space-based calorimetry, *Proc. Intl. Cosmic Ray Conference 2007 ICRC-2007* (Merida, Mexico) vol. 2, pp. 317-320
- [19] P.S. Marrocchesi et al., Active control of the gain of a  $3\text{ mm} \times 3\text{ mm}$  Silicon Photomultiplier. *Nucl.Instr. and Meth. A* 602 (2009) 391
- [20] D. Meier et al., An ASIC for SiPM/MPPC readout, *Proc. Nuclear Science Symposium and Medical Imaging Conference* 30 October – 6 November 2010, Knoxville, Tennessee (in press)
- [21] M.G. Bagliesi et al., A custom front-end ASIC for the readout and timing of 64 SiPM photosensors, *Proc. of 12th Topical Seminar on Innovative Particle and Radiation Detectors*, 7– 10 June 2010 Siena, Italy (in press)
- [22] P. von Doetinchem, et al., *Nucl. Instr. and Meth. A* 581 (2007) 151

>Secondary beta-decaying isotopes as "cosmic clocks" for Galactic cosmic-ray propagation. >Application of the FDIRC technique to the identification of cosmic-ray isotopes. >Enhanced photostatistics for nuclei of charge  $Z$  compared to particles with  $Z=1$ .